

Different topological phase transitions in the Su-Schrieffer-Heeger model under different disorder structures

Yan Gu(古燕) and Zhanpeng Lu(陆展鹏)

Citation: Chin. Phys. B, 2024, 33 (**9**): 090202. DOI: 10.1088/1674-1056/ad59fb
Journal homepage: http://cpb.iphy.ac.cn; http://iopscience.iop.org/cpb

What follows is a list of articles you may be interested in

Topological phases and edge modes of an uneven ladder

Wen-Chuang Shang(商文创), Yi-Ning Han(韩熠宁), Shimpei Endo, and Chao Gao(高超)
Chin. Phys. B, 2024, 33 (**8**): 080202. DOI: 10.1088/1674-1056/ad50c0

Effective dynamics for a spin-1/2 particle constrained to a curved layer with inhomogeneous thickness

Guo-Hua Liang(梁国华) and Pei-Lin Yin(尹佩林)
Chin. Phys. B, 2024, 33 (**2**): 020201. DOI: 10.1088/1674-1056/ad0715

Green's function Monte Carlo method combined with restricted Boltzmann machine approach to the frustrated J_1-J_2 Heisenberg model

He-Yu Lin(林赫羽), Rong-Qiang He(贺荣强), and Zhong-Yi Lu(卢仲毅)
Chin. Phys. B, 2022, 31 (**8**): 080203. DOI: 10.1088/1674-1056/ac615f

Revealing Chern number from quantum metric

Anwei Zhang(张安伟)
Chin. Phys. B, 2022, 31 (**4**): 040201. DOI: 10.1088/1674-1056/ac2f2c

Symmetry of Lagrangians of holonomic nonconservative system in event space

Zhang Bin(张斌), Fang Jian-Hui(方建会), and Zhang Wei-Wei(张伟伟)
Chin. Phys. B, 2012, 21 (**7**): 070208. DOI: 10.1088/1674-1056/21/7/070208

Different topological phase transitions in the Su–Schrieffer–Heeger model under different disorder structures

Yan Gu(古燕)[1,†] and Zhanpeng Lu(陆展鹏)[2,‡]

[1] *Shanxi Vocational University of Engineering Science and Technology, Jinzhong* 030619, *China*

[2] *Institute of Theoretical Physics and State Key Laboratory of Quantum Optics and Quantum Optics Devices, Shanxi University, Taiyuan* 030006, *China*

(Received 19 March 2024; revised manuscript received 3 June 2024; accepted manuscript online 20 June 2024)

We investigate the topological phase transition in the Su–Schrieffer–Heeger model with the long-range hopping and quasi-periodic modulation. By numerically calculating the real-space winding number, we obtain topological phase diagrams for different disordered structures. These diagrams suggest that topological phase transitions are different by selecting the specific disordered structure. When quasi-periodic modulation is applied to intracell hopping, the resulting disorder induces topological Anderson insulator (TAI) phase with high winding number ($W = 2$), but the topological states are destroyed as the disorder increases. Conversely, when intercell hoppings are modulated quasi-periodically, both TAI phase and the process of destruction and restoration of topological zero modes can be induced by disorder. These topological states remain robust even under strong disorder conditions. Our work demonstrates that disorder effects do not always disrupt topological states; rather, with a judicious selection of disordered structures, topological properties can be preserved.

Keywords: topological insulator, quasi-periodic modulation

PACS: 02.40.–k, 73.43.Nq, 73.20.At, 72.80.Ng **DOI:** 10.1088/1674-1056/ad59fb

1. Introduction

In the past decades, the search for novel topological phases of matter has been a fundamental theme.[1,2] It is well-known that topological insulators host topological invariants for bulk states and nontrivial edge modes, which have been widely explored in both condensed matter and artificial systems.[3] Generally, topological insulators are robust against weak disorder perturbations due to symmetric protection. However, under strong disorder conditions, a topological nontrivial phase of a lattice band may transition into a trivial insulator due to Anderson localization.[4–6] The Su–Schrieffer–Heeger (SSH) model stands as one of the paradigmatic examples of topological insulators, possessing two nontrivial in-gap edge states characterized by a nonzero winding number.[7] This model exhibits rich physical phenomena, such as topological soliton states[8,9] and robust edge modes.[10–13]

On the other hand, the effects of disorder are almost unavoidable in condensed matter and artificial systems. Therefore, research into localization transitions is an important topic in condensed matter physics and has been extensively studied since the pioneering work of P. W. Anderson. Anderson localization is a ubiquitous phenomenon in which the single-particle state becomes localized in a randomly disordered medium.[14,15] This phenomenon has been observed in a wide range of physical platforms, including electrons in cold atoms[16,17] and microwave cavities.[18,19] Compared with random disorder, quasi-periodic disorder can lead to exotic localization features. These features include a cascade of delocalization transitions,[20,21] and a variety of localization transitions between extended, localized, and critical states.[22,23]

Recently, great effort has been devoted to understanding the interplay of topology and disorder, which brings new perspectives. A significant breakthrough is that a disorder-induced topological phase is dubbed as topological Anderson insulator (TAI).[24,25] In addition, the TAI phase transition has been studied in various theoretical models,[26–38] it was not until 2018 that its experimental observation was reported in two different artificial systems, i.e., the one-dimensional cold atomic wires[39] and two-dimensional photonic waveguide arrays.[40] Generally, some interesting questions arise here. In particular, are the topological phase transitions in different disordered structures the same? And, what is the fate of the topological states under different disordered structures?

In this paper, we investigate the topological properties in the SSH model with long-range hopping under different disorder structures. We consider two different disorder structures. When the quasi-periodic modulation is applied to intracell hopping, the quasi-periodic disorder can induce TAI with high winding number ($W = 2$). Conversely, if the quasi-periodic modulation is applied to intercell hopping, the topological states remain robust, even in the strong disorder condition.

2. Hamiltonian

We consider an extended SSH model with quasi-periodic modulation, which can be described by the Hamiltonian

$$\mathcal{H} = \sum_{m=1} v_m (c^{\dagger}_{m,\mathrm{B}} c_{m,\mathrm{A}} + \mathrm{H.c.})$$

†Corresponding author. E-mail: guyan@sxgkd.edu.cn

‡Corresponding author. E-mail: 201712605002@email.sxu.edu.cn

© 2024 Chinese Physical Society and IOP Publishing Ltd

$$+\sum_{m=1} w_m(c^{\dagger}_{m+1,\mathrm{A}}c_{m,\mathrm{B}}+\mathrm{H.c.})$$
$$+J\sum_{m=1}(c^{\dagger}_{m+2,\mathrm{A}}c_{m,\mathrm{B}}+\mathrm{H.c.}). \quad (1)$$

The system consists of L unit cells, each containing two atoms labeled by A and B, as shown in Fig. 1. m is the index of the unit cell. $c^{\dagger}_{m,\mathrm{A}}$ ($c^{\dagger}_{m,\mathrm{B}}$) is the creation operator for a particle on the A (B) sublattice of the mth cell, and $c_{m,\mathrm{A}}$ ($c_{m,\mathrm{B}}$) is the corresponding annihilation operator. J is the long-range hopping amplitude. Here, we consider the quasi-periodic modulated intracell and intercell hopping, respectively,

$$v_m = v+\Delta_m, \quad w_m = w+\lambda_m, \quad (2)$$

with

$$\Delta_m = \Delta\cos(2\pi\beta m+\phi), \quad \lambda_m = \lambda\cos(2\pi\beta m+\phi), \quad (3)$$

where v and w are the site-independent intracell and intercell tunneling energies, Δ and λ are the strength of the quasi-periodic modulation, β is an irrational number to ensure the quasi-periodic modulation, and $\phi\in[0,2\pi)$ is an arbitrary phase. The Hamiltonian $\mathcal{H}$ satisfies the chiral symmetry with $S\mathcal{H}=-\mathcal{H}S$. Here, the chiral operator $S=I_L\otimes\sigma_z$, where σ_z is the Pauli matrix (sublattice space), and I_L is a $L\times L$ identity matrix. In the clean case ($\Delta=\lambda=0$), the long-range hopping J can lead to topological phase transition, accompanied by high winding number.[37,41,42,45] If $\Delta=\lambda=J=0$, the Hamiltonian Eq. (1) reduces to a standard SSH model. When the intracell hopping amplitude v exceeds the intercell hopping amplitude w, the system undergoes a topological phase transition accompanied by the vanishing of the zero-energy edge modes and the nontrivial winding number[7–13] under the open boundary conditions (OBCs).

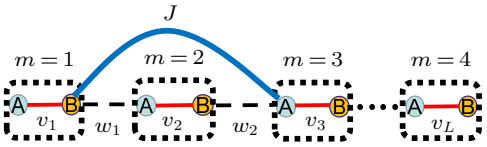


Fig. 1. Schematic of the SSH model of L unit cells. The black dotted box represents the unit cell. w_m and v_m represent the m-dependent intercell hopping and the intracell hopping, respectively. J is the long-range hopping amplitude.

In the absence of disorder, the winding number can well character the topological phase transition of the SSH model in the momentum space. If quasi-periodic modulation is introduced ($\Delta\neq0$ or $\lambda\neq0$), the system will lose translational invariance. One can apply the open-bulk winding number to character the bulk topology. The real space winding number is defined as[37,38,43,44]

$$W=\frac{1}{2L'}\mathrm{Tr}'(SQ[Q,X]), \quad (4)$$

where $X=\mathrm{diag}(1,1,2,2,\ldots,L,L)$ is the coordinate operator and $Q=\sum'_n(|\psi^n\rangle\langle\psi^n|-|\tilde{\psi}^n\rangle\langle\tilde{\psi}^n|)$. n is energy indicator and $|\tilde{\psi}^n\rangle=S|\psi^n\rangle$. The Q matrix is the homotopically equivalent flat band version of the Hamiltonian $\mathcal{H}$ under OBCs[32,37] and the chiral operator $S=\mathrm{diag}(1,-1,1,-1,\ldots,1,-1)$. To mitigate the boundary effects, the chain is divided into three intervals with lengths l, L', and l, where $L=L'+2l$. The focus of the analysis is on the middle interval with length L'. The symbol Tr' represents the trace over the middle interval length L'. W serves well for disordered systems because it does not require the translation invariance and is quantized to an integer in the limit of $L\to\infty$, while a modest size is enough in the practical calculation.

In this paper, we set w as the unit energy ($w=1$), $\beta=\frac{\sqrt{5}-1}{2}$ (golden ratio) and $\phi=0$. In the following, we will discuss the topological properties of this generalized SSH model both in the quasi-periodic modulated intracell case and the quasi-periodic modulated intercell case respectively.

3. Quasi-periodic modulated intracell case

In this section, we first explore the topological phase transition with only quasi-periodic modulated intracell hopping ($\Delta\neq0$ and $\lambda=0$).

In Fig. 2(a), we present the topological phase diagram revealed by the real-space winding number W in the J–Δ plane. As shown in Fig. 2(a), for the absence of the modulation $\Delta=0$, the system is in the clear limits and the topological phase with a high winding number $W=2$ can be induced by the long-range hopping J. With the increase of Δ, the system shows rich topological phase transitions. The topological phase diagram can be divided into three different regions, i.e., $0<J<0.35$, $0.35<J<0.65$ and $J>0.65$. When $0<J<0.35$, the system shows a topological phase transition from $W=1$ to $W=0$ by increasing Δ. For the case $J=0.3$, for small value of Δ, W keeps unit and the values of E_L and E_{L+1} remain zero, as shown in Fig. 2(b). When $\Delta>1.55$, the two zero modes E_L and E_{L+1} start to break into nonzero pairs, accompanied by the jump of the winding number W to zero, as shown in Fig. 2(b). This process indicates the topological zero modes are destroyed by disorder. For $0.35<J<0.65$, the system undergoes a transition from a topologically trivial phase to a topologically nontrivial phase, and then returns to a topologically trivial phase. A clear picture can be obtained by the winding number and the four energies as a function of Δ for $J=0.5$, as shown in Fig. 2(c). For small Δ, the system initially resides in a topologically trivial phase, corresponding to $W=0$. When $0.45<\Delta<0.8$, two pairs of topological zero modes are induced, corresponding to the TAI phase with $W=2$. When $0.8<\Delta<1.4$, one of the two pairs of zero modes disappears, accompanied by the jump of the winding number to 1. As Δ further increases, the system reverts back to the topologically trivial phase with $W=0$. For $J>0.65$, the topological phase transition for $W=2\to W=1\to W=0$ occurs by increasing Δ. For the case $J=0.3$, for small value of

Δ, two pairs of zeros modes exist and $W = 2$. As Δ increases, one of the two pairs of zero modes is destroyed, accompanied by the jump of the winding number to 1. With further increasing Δ, the two zero modes E_L and E_{L+1} start to break into nonzero pairs and the system is in the topologically trivial phase.

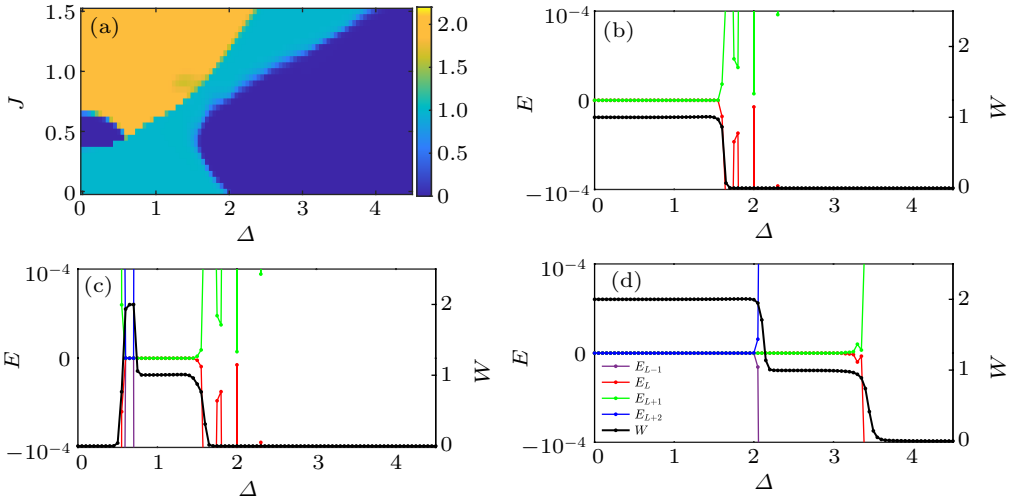


Fig. 2. (a) Topological phase diagram in the J–Δ plane. The colorbar shows the value of the winding number W. (b) Two energies E_L and E_{L+1} in the center of the spectrum, and the winding number W as a function of the modulation strength Δ under OBCs with $J = 0.3$. Four energies E_{L-1}, E_L, E_{L+1} and E_{L+2} in the center of the spectrum, and the winding number W as a function of the modulation strength Δ under OBCs with (c) $J = 0.5$ and (d) $J = 1.3$. Other parameters: $\phi = 0$ and $v = 0.64$.

4. Quasi-periodic modulated intercell case

From the previous results, we can conclude that regardless of the value of J, under the strong disorder condition, the topological states will be destroyed. In this section, we mainly discuss quasi-periodic modulated intercell case ($\lambda \neq 0$ and $\Delta = 0$). Similarly, we will mainly discuss the fate of topological states by changing the quasi-periodic modulation amplitude λ. In Fig. 3(a), we present the topological phase diagram revealed by the real-space winding number W in the J–λ plane. The topological phase diagram can also be divided into three different regions, i.e., $0 < J < 0.35$, $0.35 < J < 0.65$ and $J > 0.65$. In the region where $0 < J < 0.35$, the system is initially in a topologically nontrivial phase with $W = 1$. However, when Δ surpasses a critical value, the system transitions into the topologically trivial phase, accompanied by winding number W jumping from 1 to 0. By increasing λ, the disorder induces the emergence of the zero modes, coinciding with a sudden jump of winding number W from 0 to 1. This indicates that the zero modes can be broken and recovered with the increase of the Δ, as shown in Fig. 3(b). For $0.35 < J < 0.65$, the clean system exhibits topologically trivial characteristics. With the increase of λ, the topological zero modes emerge and winding number W jumps from 0 to 1, as shown in Fig. 3(c). This indicates that the system has undergone a TAI transition. In addition,

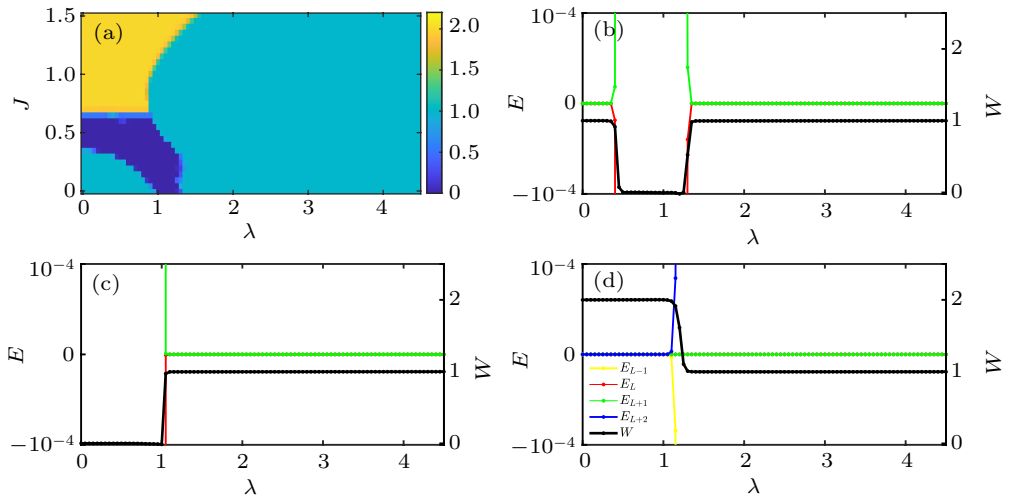


Fig. 3. (a) Topological phase diagram in the J–λ plane. The colorbar shows the value of the winding number W. Two energies E_L and E_{L+1} in the center of the spectrum, and the winding number W as a function of the modulation strength Δ under OBCs with (b) $J = 0.3$ and (c) $J = 0.5$. (d) Four energies E_{L-1}, E_L, E_{L+1} and E_{L+2} in the center of the spectrum, and the winding number W as a function of the modulation strength λ under OBCs with $J = 1.3$. Other parameters: $\phi = 0$ and $v = 0.64$.

W keeps unit by increasing λ. For $J > 0.65$, two pairs of zero modes exhibit, corresponding to $W = 2$. When $\lambda > 1.1$, one of the two pairs of edge modes disappears, accompanied by the jump of the winding number to 1, as shown in Fig. 3(d) for $J = 1.3$. One can see that the two zero modes E_L and E_{L+1} never break into nonzero pairs, even in strong disorder situation. If disorder averaging is considered, the conclusion remains unchanged. See Appendix A for the results.

To more directly reflect the changes in the topological state, we plotted the spatial distribution of the eigenfunctions corresponding to the middle four energy levels at two parameter points ($\lambda = 0.8$ and 1.5) around the topological phase transition point. For a clear comparison, we included the variation of W with disorder strength λ, as shown in Fig. 4(a). In Fig. 4(b), it can be observed that when $\lambda = 0.8$, the eigenfunctions corresponding to the middle four energy levels are all topological edge states. There should be two pairs of degenerate zero modes in the system, and the corresponding winding number $W = 2$, which is consistent with the results in Fig. 4(a). However, when $\lambda = 1.5$, as shown in Fig. 4(c), two of the eigenfunctions corresponding to the middle four energy levels are disrupted by the disorder, leaving only two topological edge states. In this case, there is only one pair of degenerate zero modes in the system, and the corresponding winding number $W = 1$, which is also consistent with the results in Fig. 4(a).

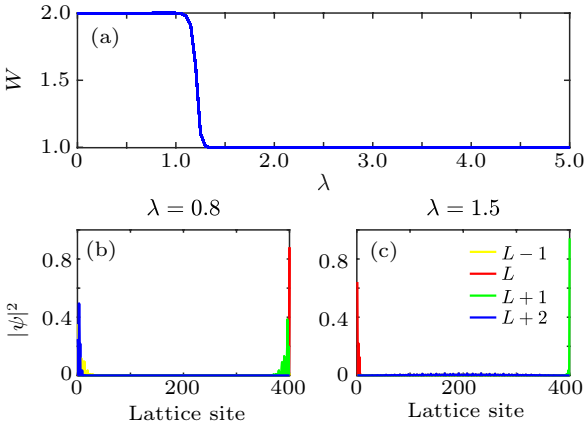


Fig. 4. (a) The winding number W as a function of the modulation strength λ under OBCs with $J = 1.3$. Wave function distribution of the middle four energies E_{L-1}, E_L, E_{L+1} and E_{L+2} with (b) $\lambda = 0.8$ and (c) $\lambda = 1.5$. Other parameters: $L = 200$, $\phi = 0$ and $v = 0.64$.

5. Conclusion

To conclude, we studied TAI in SSH model with long-range hopping under different disorder structures. In quasi-periodic modulated intracell case, we find the TAI phases with high winding number $W = 2$ can be induced by disorder. The topological phase only exists in a finite range with the increase of disorder. In quasi-periodic modulated intercell case, TAI with $W = 1$ can be induced. In a specific parameter range of J, the topological zero modes exhibit a process of destruction followed by restoration with increasing disorder. We find the topological states robust against strong disorder perturbation. These results indicate that disorder does not always disrupt the topological states; instead, the judicious selection of disordered structures can help preserve the topological states. If another value of β is considered, the conclusion remains unchanged. See Appendix B for the results.

Appendix A: Disorder-averaged topological phase diagram

In this appendix, we present the disorder-averaged topological phase diagram. Furthermore, we define the disorder-averaged winding number $\overline{W} = 1/N_c \sum_{c=1}^{N_c} W$ is the number of the disorder realization by choosing different phases ϕ. Here, we consider $N_c = 20$.

Figures A1(a) and A1(b) show topological phase diagrams of quasi-periodic modulated intracell case and intercell case, respectively. From Figs. A1(a) and A1(b), the results show that disorder averaging has little impact on the topological phase diagram.

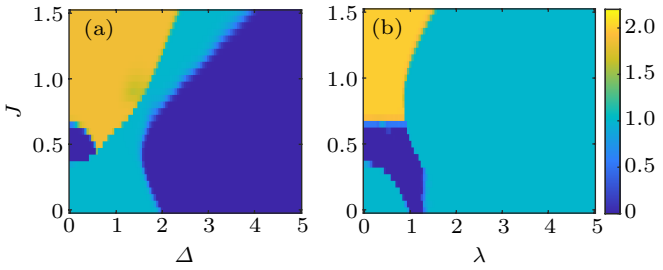


Fig. A1. (a) Topological phase diagram in the J–Δ plane with quasi-periodic modulated intracell case. (b) Topological phase diagram in the J–λ plane with quasi-periodic modulated intercell case. The colorbar shows the value of the disorder-averaged winding number $\overline{W}$. Other parameters: $L = 200$, $N_c = 20$ and $v = 0.64$.

Appendix B: $\beta = \sqrt{2} - 1$

In this appendix, we present the topological phase diagram with $\beta = \sqrt{2} - 1$. Figures B1(a) and B1(b) show the topological phase diagrams of quasi-periodic modulated intracell case and intercell case, respectively. From Fig. B1(a),

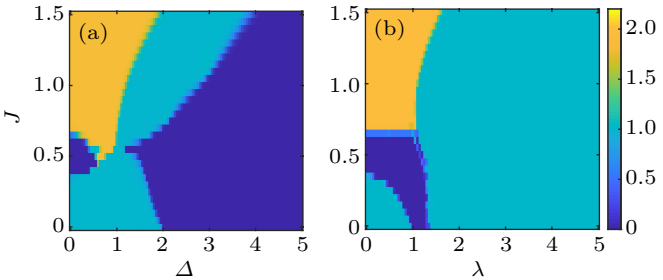


Fig. B1. (a) Topological phase diagram in the J–Δ plane with quasi-periodic modulated intracell case. (b) Topological phase diagram in the J–λ plane with quasi-periodic modulated intercell case. The colorbar shows the value of the winding number W. Other parameters: $L = 200$, $\beta = \sqrt{2} - 1$, $\phi = 0$ and $v = 0.64$.

the results show that when quasi-periodic modulation is applied to intracell hopping, the resulting disorder induces TAI phase with high winding number, but the topological states are destroyed as the disorder increases. Conversely, Fig. B1(b) shows that when intercell hoppings are modulated quasi-periodically, these topological states remain robust, even under strong disorder conditions.

Acknowledgements

Project supported by the National Natural Science Foundation of China (Grant No. 12205176) and the High-level Talent Research Start-up Project (Grant No. RCK202231).

References

[1] Thouless D J, Kohmoto M, Nightingale M P and Nijs M D 1982 *Phys. Rev. Lett.* **49** 405
[2] Hasan M Z and Kane C L 2010 *Rev. Mod. Phys.* **82** 3045
[3] Qi X L and Zhang S C 2011 *Rev. Mod. Phys.* **83** 1057
[4] Bansil A, Lin H and Das T 2016 *Rev. Mod. Phys.* **88** 021004
[5] Chiu C K, Teo J C Y, Schnyder A P and Ryu S 2016 *Rev. Mod. Phys.* **88** 035005
[6] Armitage N P, Mele E J and Vishwanath A 2018 *Rev. Mod. Phys.* **90** 015001
[7] Su W P, Schrieffer J R and Heeger A J 1979 *Phys. Rev. Lett.* **42** 1698
[8] Jackiw R and Rebbi C 1976 *Phys. Rev. D* **13** 3398
[9] Heeger A J, Kivelson S, Schrieffer J R and Su W P 1988 *Rev. Mod. Phys.* **60** 781
[10] Ganeshan S, Sun K and Sarma S D 2013 *Phys. Rev. Lett.* **110** 180403
[11] Song F, Yao S and Wang Z 2019 *Phys. Rev. Lett.* **123** 246801
[12] Xu Z, Zhang R, Chen S, Fu L and Zhang Y 2020 *Phys. Rev. A* **101** 013635
[13] Xiao T, Xie D, Dong Z, Chen T, Yi W and Yan B 2021 *Sci. Bull.* **66** 2175
[14] Anderson P W 1958 *Phys. Rev.* **109** 1492
[15] Lee P A and Ramakrishnan T V 1985 *Rev. Mod. Phys.* **57** 287
[16] Billy J, Josse V, Zuo Z, Bernard A, Hambrecht B, Lugan P, Clément D, Sanchez-Palencia L, Bouyer P and Aspect A 2008 *Nature* **453** 891
[17] Roati G, D'Errico C, Fallani L, Fattori M, Fort C, Zaccanti M, Modugno G, Modugno M and Inguscio M 2008 *Nature* **453** 895
[18] Chabanov A A, Stoytchev M and Genack A Z 2000 *Nature* **404** 850
[19] Pradhan P and Sridhar S 2000 *Phys. Rev. Lett.* **85** 2360
[20] Goblot V, Štrkalj A, Pernet N, Lado J L, Dorow C, Lemaître A, Gratiet L L, Harouri A, Sagnes I, Ravets S, Amo A, Bloch J and Zilberberg O 2020 *Nat. Phys.* **16** 832
[21] Zhai L J, Huang G Y and Yin S 2021 *Phys. Rev. B* **104** 014202
[22] Wang Y, Zhang L, Sun W, Poon T F J and Liu X J 2022 *Phys. Rev. B* **106** L140203
[23] Ahmed A, Ramachandran A, Khaymovich I M and Sharma A 2022 *Phys. Rev. B* **106** 205119
[24] Li J, Chu R L, Jain J K and Shen S Q 2009 *Phys. Rev. Lett.* **102** 136806
[25] Groth C W, Wimmer M, Akhmerov A R, Tworzydlo J and Beenakker C W J 2009 *Phys. Rev. Lett.* **103** 196805
[26] Guo H M, Rosenberg G, Refael G and Franz M 2010 *Phys. Rev. Lett.* **105** 216601
[27] Zhang Y Y, Chu R L, Zhang F C and Shen S Q 2012 *Phys. Rev. B* **85** 035107
[28] Song J, Liu H, Jiang H, Sun Q F and Xie X C 2012 *Phys. Rev. B* **85** 195125
[29] Girschik A, Libisch F and Rotter S 2013 *Phys. Rev. B* **88** 014201
[30] Mondragon-Shem I, Hughes T L, Song J and Prodan E 2014 *Phys. Rev. Lett.* **113** 046802
[31] Zhang Z Q, Wu B L, Song J and Jiang H 2019 *Phys. Rev. B* **100** 184202
[32] Zhang D W, Tang L Z, Lang L J, Yan H and Zhu S L 2020 *Sci. China Phys. Mech. Astron.* **63** 267062
[33] Tang L Z, Zhang L F, Zhang G Q and Zhang D W 2020 *Phys. Rev. A* **101** 063612
[34] Zhang G Q, Tang L Z, Zhang L F, Zhang D W and Zhu S L 2021 *Phys. Rev. B* **104** L161118
[35] Liu S N, Zhang G Q, Tang L Z and Zhang D W 2022 *Phys. Lett. A* **431** 128004
[36] Wu Y P, Tang L Z, Zhang G Q and Zhang D W 2022 *Phys. Rev. A* **106** L051301
[37] Zhang W J, Wu Y P, Tang L Z and Zhang G Q 2022 *Commun. Theor. Phys.* **74** 075702
[38] Tang L Z, Liu S N, Zhang G Q and Zhang D W 2022 *Phys. Rev. A* **105** 063327
[39] Meier E J, An F A, Dauphin A, Maffei M, Massignan P, Hughes T L and Gadway B 2018 *Science* **362** 929
[40] Stützer S, Plotnik Y, Lumer Y, Titum P, Lindner N H, Segev M, Rechtsman M C and Szameit A 2018 *Nature* **560** 461
[41] Hsu H C and Chen T W 2020 *Phys. Rev. B* **102** 205425
[42] Song J and Prodan E 2014 *Phys. Rev. B* **89** 224203
[43] Song F, Yao S and Wang Z 2019 *Phys. Rev. Lett.* **123** 246801
[44] Kitaev A 2006 *Ann. Phys.* **321** 2
[45] Malakar R K and Ghosh A K 2023 *J. Phys.: Condens. Matter* **35** 335401